OXFORD

Cerebral Cortex, 2015, 1–8

doi: 10.1093/cercor/bhv280
Original Article

ORIGINAL ARTICLE

Evidence for Competition for Target Innervation in the Medial Prefrontal Cortex

Ramon Guirado[1], Juzoh Umemori[1], Pia Sipilä[1,2] and Eero Castrén[1]

[1]Neuroscience Center, University of Helsinki, Helsinki, Finland and [2]Current address: Max Planck Institute for Neurobiology, Martinsried, Germany

Address correspondence to Ramon Guirado, Neuroscience Center, University of Helsinki, Viikinkaari 4, 00790 Helsinki, Finland.
Email: ramon.guirado@helsinki.fi; Eero Castrén, Neuroscience Center, University of Helsinki, Viikinkaari 4, 00790 Helsinki, Finland. Email: eero.castren@helsinki.fi

Abstract

Inputs to sensory cortices are known to compete for target innervation through an activity-dependent mechanism during critical periods. To investigate whether this principle also applies to association cortices such as the medial prefrontal cortex (mPFC), we produced a bilateral lesion during early development to the ventral hippocampus (vHC), an input to the mPFC, and analyzed the intensity of the projection from another input, the basolateral amgydala (BLA). We found that axons from the BLA had a higher density of "en passant" boutons in the mPFC of lesioned animals. Furthermore, the density of neurons labeled with retrograde tracers was increased, and neurons projecting from the BLA to the mPFC showed increased expression of FosB. Since neonatal ventral hippocampal lesion has been used as an animal model of schizophrenia, we investigated its effects on behavior and found a negative correlation between the density of retrogradely labeled neurons in the BLA and the reduction of the startle response in the prepulse inhibition test. Our results not only indicate that the inputs from the BLA and the vHC compete for target innervation in the mPFC during postnatal development but also that subsequent abnormal rewiring might underlie the pathophysiology of neuropsychiatric disorders such as schizophrenia.

Key words: basolateral amygdala, critical period, medial prefrontal cortex, network, schizophrenia

Introduction

The groundbreaking work of Hubel and Wiesel in the visual cortex demonstrated that major input projections compete for target innervation during critical periods through activity-dependent plasticity (Hubel and Wiesel 1970). Further studies have extended these principles to other sensory areas of the brain such as the somatosensory (Van der Loos and Woolsey 1973) or the auditory cortices (Harrison et al. 1993). It remains unknown whether this principle also applies to other higher cognitive areas such as the medial prefrontal cortex (mPFC). However, the presence of partially overlapping columnar-like structures in the monkey frontal association cortex (Goldman-Rakic and Schwartz 1982) suggests that competition for target innervation might be a general principle of cortical organization.

While in the primary sensory areas, the information input is well known and easy to experimentally manipulate (monocular deprivation, whisker trimming, etc.), in higher cognitive areas such as the mPFC multiple associative inputs exist, making studying these same principles difficult. Nevertheless, several studies have reported in detail the input connectivity of the mPFC (Gabbott et al. 1997, 2005; Hoover and Vertes 2007). Two of the brain areas projecting to the mPFC are the basolateral complex of the amygdala (BLA) and the ventral part of the hippocampus (vHC). Both regions send glutamatergic projections, which monosynaptically contact both pyramidal neurons (Jay et al. 1989; Carr and Sesack 1996) and interneurons (Gabbott et al. 2002; Tierney et al. 2004) in the mPFC.

The BLA is an important region for emotion-related behavioral phenotypes, and its role has been extensively studied in fear conditioning, aggression and schizophrenia animal models (Garcia et al. 1999; Laviolette et al. 2005; Sierra-Mercado et al. 2010; Toth et al. 2012). On the other hand, the vHC has been linked to spatial learning and memory (Kjelstrup et al. 2008) and emotional behaviors (Strange et al. 2014). In fact, its activity has been suggested to disrupt fear expression behaviors (Sotres-Bayon et al. 2012) and to promote extinction through context-dependent learning (Corcoran et al. 2005; Ji and Maren 2007).

We hypothesize that pyramidal neurons in the mPFC integrate these competing types of information, providing a top-down control of spatial and affective processes (Ressler and Mayberg 2007; Fuster 2009; Arnsten et al. 2012) in a similar fashion as the visual cortex integrates information from left and right eyes (Levelt and Hübener 2012): an activity-dependent competition for target innervation during a critical period, which would shape mPFC connectivity.

To investigate this principle, we produced a lesion in the vHC during early postnatal development and studied the effects on the projection from the BLA to the mPFC in the adult brain. We show that lesions in the vHC lead to a strengthening in the projection from the BLA to the mPFC, which is consistent with the idea that projections from hippocampus and amygdala compete for innervation in the prefrontal cortex. Finally, since this lesion protocol has been considered as an animal model of schizophrenia (Lipska et al. 1993), these results suggest that the strength of the projection from amygdala might underlie the pathophysiology of this disorder. In fact, we found a negative correlation between the strength of the projection between from the BLA to the mPFC and the reduction of the startle response, a sensorimotor-gating test usually considered for evaluating schizophrenic-like behaviors (Geyer et al. 2001).

Materials and Methods

Animals

A total of 32 Long-Evans rats were used for the study ($n = 16$). A first generation of breeders were obtained from Harlan, and they were bred in our animal facility, where they were maintained in standard conditions of light and temperature, with no limit in the access to food and water. All experiments were conducted according to the guidelines of the European Council Directive (86/609/EEC) and were approved by the County Administrative board of Southern Finland. Every effort was made to minimize the number of animals used and their suffering.

Lesions in the vHC

At postnatal age of 7 days, pups were anesthetized using isoflurane (induction with 4% and afterwards 1–1.5%) and then placed in a stereotaxic frame. Then, we injected 0.3 µL of ibotenic acid (10 µg/µL; Abcam) in the vHC: AP—3.0 mm and ML ± 3.5 mm relative to Bregma, and DV—5.0 mm, as described by Lipska et al. 1993. We injected using a microinjector (Stoelting) at a rate of 0.15 µL/min (2 min) and then waited 4 min before carefully lifting the Hamilton syringe. A similar number of pups from the same litter were distributed to either neonatal ventral hippocampal lesion (NVHL) or control groups, which in turn were injected with phosphate-buffered saline (PBS) as vehicle solution. A total of 16 pups from 5 different litters were included in each group. Animals were weaned at postnatal day 21 and were kept in groups of 3–4 animals per cage. Handling of animals, apart from cage changes and surgical procedures, was avoided.

Behavior

At postnatal day 70, animals were individually placed in 42 × 42 × 31-cm behavioral chambers for 60 min (Accuscan activity monitor, Columbus). The monitor contained 16 horizontal and 8 vertical infrared sensors spaced 2.5 cm apart. Locomotor activity was calculated using the number of beams broken by the animals after placement in the chamber. We measured the total distance traveled over the 60 min in 5-min intervals. The data were analyzed using repeated measures two-way ANOVA, being time and the lesion the factors analyzed, followed by Sidak's multiple comparison test.

The next day, rats were placed in an elevated plus maze. The maze consisted of 2 open arms (50 × 10 cm) and 2 closed arms (50 × 10 cm) connected by a central platform (10 × 10 cm) and elevated 50 cm above the floor. The maze was made of gray plastic, and the closed arms were surrounded by opaque side- and end-walls (40 cm high). The room was illuminated by fluorescent ceiling lights (~100 lx). The rat was placed in the center of the maze facing one of the enclosed arms and observed for 5 min. Behavior was tracked and analyzed by Noldus EthoVision XT 10 system (Noldus Information Technology). The latency to the first open arm entry, number of open and closed arm entries (4-paw criterion), the time spent and distance traveled in different zones of the maze were measured. Data were analyzed using unpaired *t*-test.

Finally, due to the importance of sensorimotor gating as standard evaluation in animal models of schizophrenia, the next day rats went through a prepulse inhibition (PPI) test: Rats were enclosed in a transparent plastic tube (Ø 4.5 cm, length 8 cm) that was placed in the startle chamber (Med Associates) with a background white noise of 65 dB and left undisturbed for 5 min. Testing was performed in 12 blocks of 5 trials, and 5 trial types were applied. One trial type was a 40-ms, 120-dB white noise acoustic startle stimulus (SS) presented alone. In the remaining 4 trial types, the SS was preceded by the acoustic prepulse stimulus (PPS). The 20-ms PPS were white noise bursts of 68, 72, 76 and 80 dB. The delay between onset of PPS and SS was 100 ms. The 1st and 12th block consisted of SS-alone trials. In remaining blocks, the SS and PPS + SS trials were presented in pseudorandomized order such that each trial type was presented once within a block of 5 trials. The intertrial interval ranged between 10 and 20 s. The startle response was recorded for 65 ms starting with the onset of the SS. The maximum startle amplitude recorded during the 65-ms sampling window was used as the dependent variable. The startle response was averaged over 10 trials from blocks 2–11 for each trial type. The PPI for each PPS was calculated by using the following formula: 100-[(startle response on PPS + SS trials/startle response on SS trials) × 100]. Data were afterwards analyzed using unpaired *t*-test.

Tracing

Eight female rats (4 per group) were injected with an adeno-associated virus (AAV6-CAG-EGFP; SignaGen) in the left hemisphere 2 weeks before the first behavioral test. This virus was used as anterograde tracer, since the axons of the infected neurons display clear GFP expression in the axons. Animals were placed in a stereotaxic frame under isoflurane anesthesia (4% induction, 2% surgery). Then, using a microinjector, we infused the virus in the left BLA: AP—3.3 mm and ML + 2.0 mm relative to Bregma and DV—8.5 mm with an angle of −19° relative to the brain surface.

Sixteen male rats (8 per group) were injected bilaterally with a retrograde tracer (Retrobeads, Lumafluor) 3 days after the last behavioral test. Using a microinjector, animals were intracerebrally injected 1 µL of the tracer (rate of 0.2 µL per minute) in the

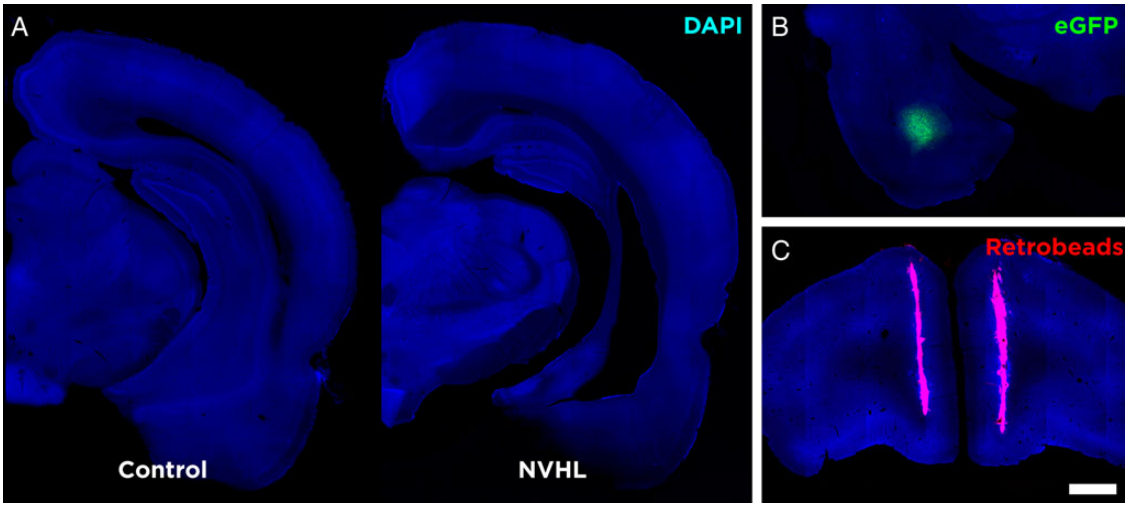

Figure 1. Evaluation of the lesions and intracerebral injections. (*A*) Confocal plane of DAPI staining in animals injected with vehicle and ibotenic acid, showing the extent of the lesion in the vHC. (*B*) Confocal plane showing eGFP expression in the basolateral amygdala 3 weeks after the injection with the virus. (*C*) Confocal plane showing the injection site of the retrograde tracer (red retrobeads). Scale bar = 1 mm.

prelimbic area (PrL) of the mPFC (mPFC): AP + 2.7 mm and ML ± 0.5 mm relative to Bregma and DV—3.6 mm relative to the brain surface. However, since our injections covered also partially the infralimbic (IL) area, we will consider the injections to be located in the IL/PrL region.

Perfusion

Four days after the injection of the retrograde tracer (1 week after the last behavioral experiment), animals were perfused transcardially under deep pentobarbital anesthesia, first with saline and then with PFA 4% in PB 0.1 M. After perfusion brains were extracted and postfixed in the same fixative solution for 2 h and then stored in PB 0.1 m with sodium azide 0.05%. Then, brains were cut into 60-µm sections using a vibratome (VT 1000E, Leica). Sections were collected in 7 subseries and stored at 4°C in PB 0.1 m and sodium azide. Sections were then washed in PB 0.1 m and mounted on slides and coverslipped using fluorescence mounting medium with DAPI (Fluoroshield, Abcam).

Immunohistochemistry

Tissue was processed free-floating for fluorescence immunohistochemistry. Sections were washed in PBS, and then slices were incubated in 10% normal goat serum (NGS; Gibco), 0.2% Triton X-100 (Sigma) in PBS for 1 h. Sections were then incubated for 48 h at 4°C with different cocktails containing combinations of the following primary antibodies: IgG mouse anti-CAMKII (1:500 dilution; Millipore), IgG rabbit anti-PV (1:2000; Swant), IgG rabitt anti-FosB (1:500; Santa Cruz), and IgY chicken anti-GFP (1:1000; Abcam) antibodies diluted in PBS 0.2% Triton X-100. After washing again, sections of animals were incubated for 2 h at room temperature with cocktail containing different secondary antibodies: anti-mouse conjugated with Alexa 647, anti-rabbit conjugated with Alexa 546 or Alexa 488, and anti-chicken conjugated with A488 antibodies (1:200; Life Technologies). Finally, sections were washed in PB 0.1 m, mounted on slides, and coverslipped using fluorescence mounting medium (Dako).

Imaging

We used DAPI to precisely define the cytoarchitecture of the brain parenchyma and to determine the extent of the lesion in the vHC and the location of the BLA and the mPFC. Only animals with a complete lesion of the vHC and comparable tracer injections were used for the study (with the retrograde tracer $n = 8$ NVHL animals and 5 for the control group and with the anterograde virus 3 each group).

Retrograde labeling in the amygdala was analyzed using images taken at 400× magnification (Olympus BX41) where the number of tagged neurons containing the Retrobeads was counted and compared using unpaired *t*-test. For the anterograde labeling from the amygdala, 2/3 different sections (from AP +2.2 to +3.2 mm relative to Bregma) in the mPFC were analyzed. Two stacks per section were obtained at high magnification and then axons longer than 60 µm (up to 180 µm; average axonal length analyzed per animal in IL and PrL was 110 and 120 µm, respectively) and with clear fluorescence were randomly selected within the images; we counted the number of axonal boutons and analyzed it using unpaired *t*-test, using the number of axons as *n*. Varicosities that were at least twice thicker and 3 times more intensily fluorescent than the internodal segments were counted as "en passant" boutons. A nonparametric Spearman correlation analysis was used for the correlation between the density of retrograde-labeled neurons and the reduction in the startle response in the PPI.

For the FosB quantification, confocal stacks were obtained, and then neurons located at the same depth of the section were analyzed. We run a two-way ANOVA, the depth within the tissue and lesions were the 2 factors analyzed. We found that both factors were significant. These results show that depth was an important factor to take into account as fluorescence decreases with the depth. Therefore, we performed multiple comparison test with Sidak's post hoc to compare changes in fluorescence intensity at 3 different ranges of depth (0–5, 6–10, and 11–15 µm). We found changes in the comparison at the surface of the tissue (data shown). All animals were coded, and the code was not broken until the end of the study.

Results

To create an imbalance between 2 inputs to the mPFC, we used NVHLs and investigated the effects of this lesion to the innervation of the mPFC by neurons within the BLA. Injection of

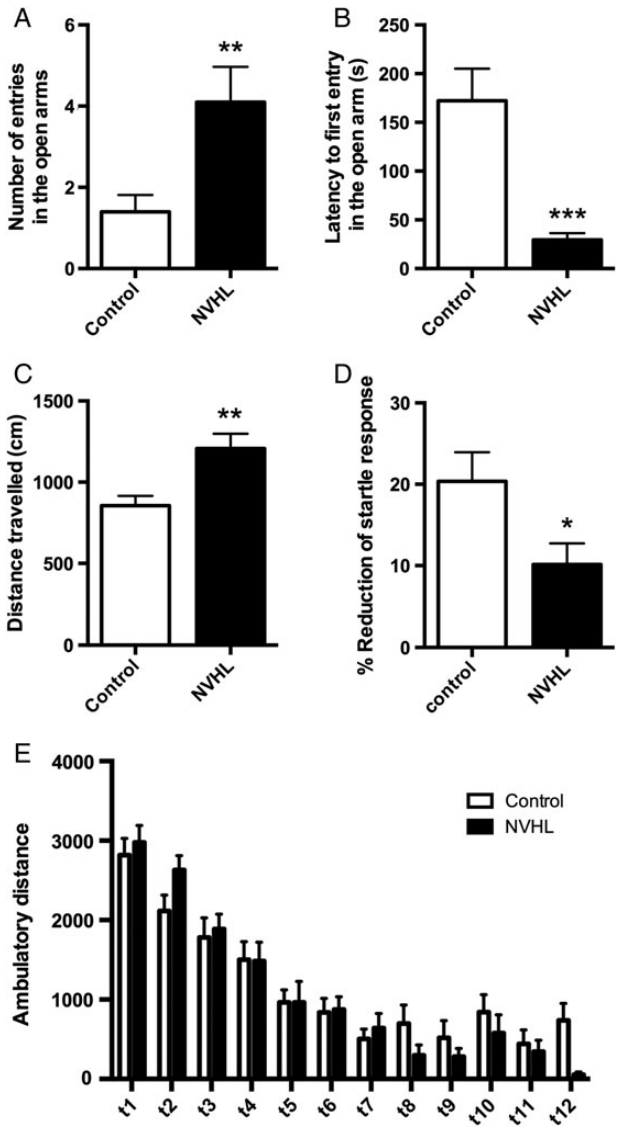

Figure 2. NVHL produces behavioral changes in the adulthood. (*A*) Graphs showing the number of entries in the open arms, (*B*) the latency in seconds to the first entry to the open arms, and (*C*) the distance traveled in centimeters in the elevated plus maze. (*D*) Graphs showing the reduction of the startle response with a prepulse of 68 dB in the PPI test. (*E*) Graphs showing the ambulatory distance in the locomotor activity cages (t1, t2, etc. stands for time periods of 5 min each; RM two-way ANOVA with Sidak's multiple comparison test) (*t*-test; *P*-values: *<0.05, **<0.01, and ***<0.001). Bars represent means ± standard error of the mean (SEM), $n = 15$ for the control group and 12 for the NVHL group (number of animals).

ibotenic acid into the vHC of rats at postnatal day 7 produces a substantial lesion within the vHC as observed in the adulthood (Fig. 1A). NVHL paradigm has previously been used as an animal model of schizophrenia, leading to a distinct phenotype showing reduced anxiety and abnormalities in sensorimotor gating. Therefore, we first studied behavioral consequences of NVHL to validate our lesions.

In the elevated plus maze, we found a significant increase in the number of entries in the open arms in the NVHL group ($P = 0.006$; Fig. 2A). The latency time until the first entry in the open arms was significantly reduced in the lesion animals ($P < 0.001$; Fig. 2B). In addition, we observed an increase in the total distance traveled of the lesion animals ($P = 0.003$; Fig. 2C). These data are consistent with previous reports (Lipska et al. 1993; Sandner et al. 2011).

In the PPI test, also as previously reported (Lipska et al. 1995; Le Pen and Moreau 2002), the NVHL group showed significantly lower reduction in the amplitude of the startle response with low-intensity prepulses (68 dB; $P = 0.030$; Fig. 2D). Finally, we also studied locomotor activity and we did not find any significant effect of NVHL (Fig. 2E).

The main goal of this study was to analyze the effect of a lesion in the vHC on the intensity of the projection from the BLA to the mPFC (mPFC). We injected an adeno-associated virus transfecting the eGFP into the BLA (Fig. 1B) and analyzed the density of axonal boutons in the mPFC. We observed 2 clear bands of high density of axons from that projection as described before (Gabbott et al. 2006), one at the Layer II and another at Layer V in both the IL and PrL areas (Fig. 3A). We investigated the neurochemical phenotype of the neurons contacted by the axonal boutons from this projection in both layer V (Fig. 3B) and Layer II (Fig. 3C). CAMKII-expressing neurons (hash in Fig. 3B and C) appear to be the main target of the axons projecting from the BLA. However, we also found that parvalbumin (PV)-expressing interneurons in Layer V (asterisk in Fig. 3B and C) are surrounded by overlapping axonal boutons (Fig. 3B1), suggesting synaptic contacts whereas they lack this apparent innervation in Layer II (Fig. 3C1).

We observed that animals with the lesion had an increased density of boutons in the axons from the BLA reaching the Layer V of the PrL cortex ($P = 0.015$; Fig. 4C) whereas interestingly, the opposite was found in the same layer of the IL cortex, with a significant reduction in the density of axonal boutons ($P = 0.005$; Fig. 4D). When we then analyzed the connectivity of projections from the amygdala reaching Layer II in both PrL and IL, we found a significant increase in the density of axonal boutons from the BLA in both of these prefrontal cortical areas ($P = 0.013$ and 0.034, respectively).

To investigate whether neuronal activity might be increased in the BLA neurons projecting to the mPFC in the NVHL rats, we analyzed the intensity of FosB expression, a long-term activity marker (Gabbott et al. 2005; Hale et al. 2008; Marchant et al. 2010, 2014; Vázquez-Borsetti et al. 2011) in the BLA. We show that in NVHL animals, neurons projecting to the mPFC, labeled with the retrograde tracers, showed increased FosB expression ($P = 0.011$; Fig. 5C) when compared with neurons in the amygdala of control rats.

As another indicator of the strength of the projection, we studied the density of neurons in the BLA tagged with a retrograde tracer injected in the mPFC (Fig. 1C). We observed that animals from the NVHL group (Fig. 5B) had a significantly higher number of neurons tagged when compared with the control group ($P = 0.032$; Fig. 5A and D). We also confirmed that the retrograde-labeled neurons in the BLA are excitatory neurons expressing CAMKII (Fig. 5B1).

Finally, we investigated a possible correlation between the performance of the animals in the PPI test, and the strength of the amygdalar projection in animals injected with vehicle and with ibotenic acid together. We found a significant negative correlation between those factors: the stronger the intensity of the amygdalar projection, the weaker the reduction of the startle response ($r = -0.610$ and $P = 0.030$; Fig. 5E).

Discussion

In the present study, we demonstrate that a lesion in the vHC at early postnatal life leads to an increased strength of the projection from the BLA to the mPFC in terms of density of "en passant"

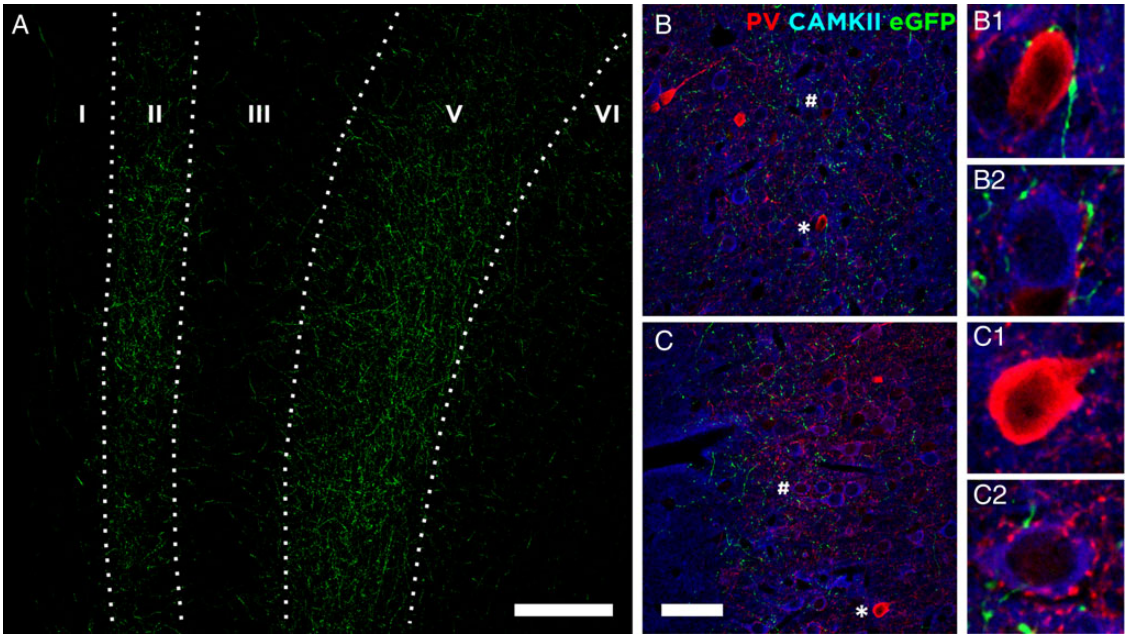

Figure 3. Characterization of the projection from the BLA to the mPFC. (*A*) Low-magnification confocal image showing the axonal collaterals in the PrL region mainly innervating Layers II and V. (*B*) Confocal plane showing the expression of eGFP in green, parvalbumin in red, and CAMKII in blue in Layer V and (*C*) Layer II of PrL. (B1 and C1) Insets showing in detail a parvalbumin-expressing interneuron. Asterisks indicate the soma of PV interneurons (shown in B1 and C1). Hashes indicate the soma of CAMKII neurons (shown in B2 and C2). Scale bar = 200 µm in A and 50 µm in B.

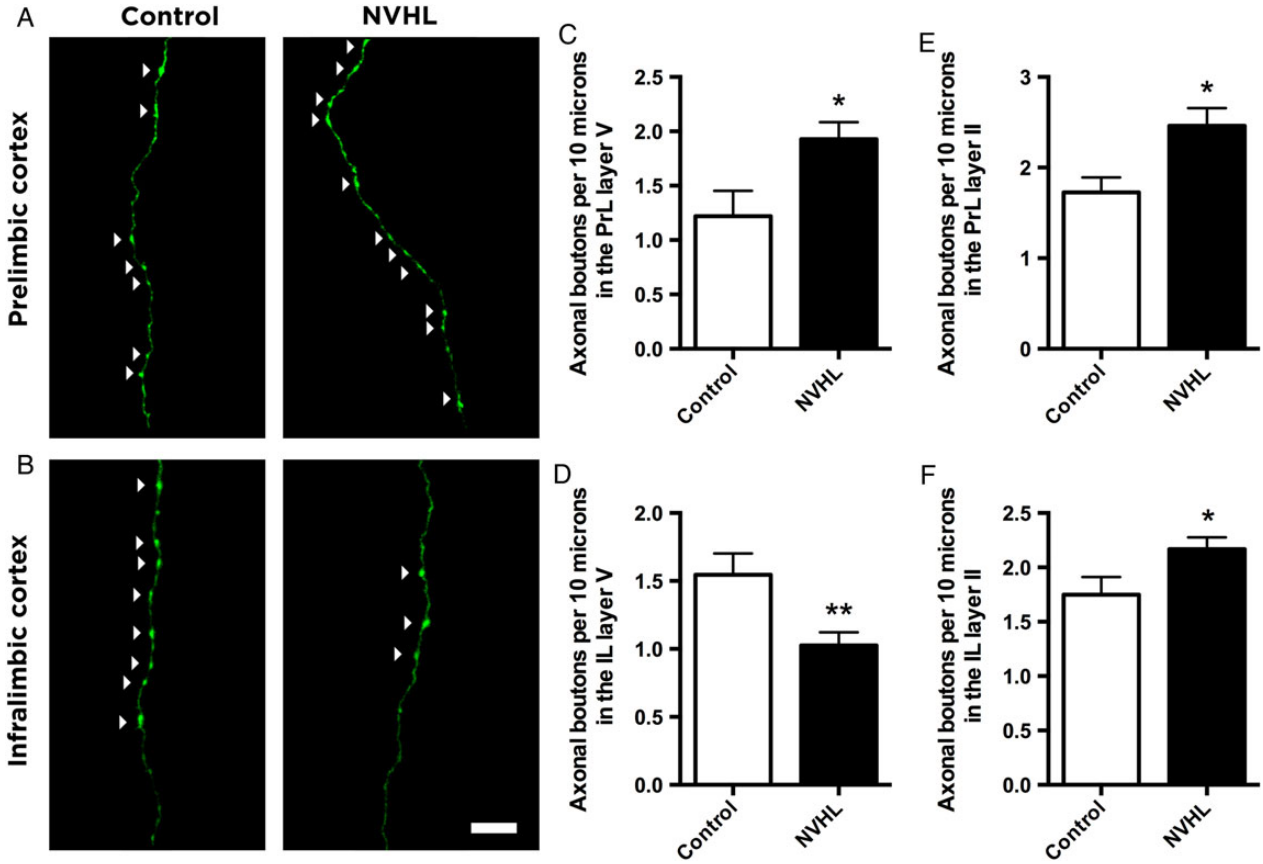

Figure 4. Analysis of the anterograde tracing. (*A*) Reconstruction of confocal planes showing differences in "en passant" boutons in axonal segments from the BLA (BLA) of control and NVHL animals in Layer V of the PrL cortex and (*B*) IL cortex. (*C*) Graphs showing the density of axonal boutons per 10 µm in Layer V of PrL and (*D*) IL, and Layer II of PrL (*E*) and IL (*F*). Bars represent means ± SEM, $n = 9$ for the control group and 15 for the NVHL group (number of axons). Scale bar = 10 µm (*t*-test; *P*-values: *<0.05 and **<0.01).

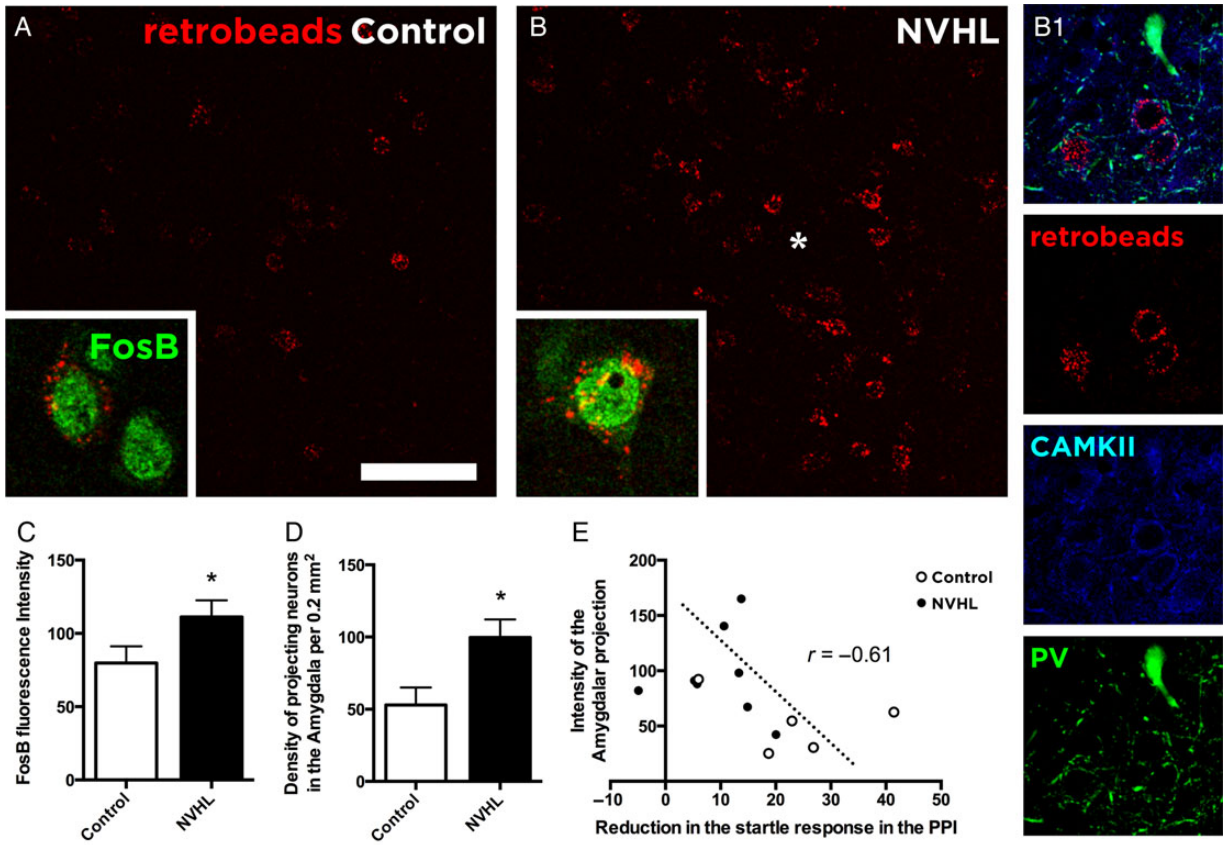

Figure 5. Analysis of the retrograde tracing from the mPFC. Confocal planes showing neurons labeled with red Retrobeads in the BLA of (*A*) control and (*B*) NVHL animals. Insets showing representative confocal planes of FosB expression in neurons labeled with the retrobeads. (B1) Confocal plane showing the co-localization of parvalbumin in green, CAMKII in blue, and the red Retrobeads in the BLA. (*C*) Graph showing the FosB fluorescence intensity in Control and NVHL animals. (*D*) Graph showing the density of neurons per 0.2 mm^2 labeled with the retrograde tracer in the BLA (*t*-test; *P*-values: *<0.05). Bars represent means ± SEM, $n = 5$ for the control group and 9 for the NVHL group (number of animals). (*E*) Graph showing the correlation between the density of labeled neurons in the BLA and the reduction in the startle response in the PPI test (Spearman correlation; $r = -0.61$ and $P = 0.03$). Scale bar = 100 µm.

boutons of the axons, density of neurons tagged with a retrograde tracer and their expression levels of FosB. This lesion covers a time-window that has been previously shown to be important for the network plasticity involved in NVHL (Lee et al. 2012).

Activity-dependent competition for target innervation drives the connectivity and structure of sensory areas in the neocortex during sensitive periods (Fox 1992; Berardi et al. 2000; Hensch 2004). In primary sensory cortices, producing an imbalance of inputs is experimentally easy (whisker trimming, eyelid suture, etc.). However, in the present study, we investigate whether that same principle also applies in higher cognitive areas such as the mPFC. In order to weaken one of the inputs of the Mpfc, we performed a lesion in the vHC during early development (Lipska et al. 1993, 1995).

The vHC sends glutamatergic projections to the mPFC, providing spatial and sensory information to that region (Sotres-Bayon et al. 2012). These axon terminals are in close proximity to axon terminals arising from the BLA (Bacon et al. 1996). Both projections have been reported to innervate both CAMKII-expressing pyramidal neurons and PV-expressing interneurons, as we observe here in our study (Carr and Sesack 1996; Gabbott et al. 2002, 2006). Therefore, the same neurons in the mPFC could integrate spatial information provided by the hippocampus (Spellman et al. 2015) and emotional information from the amygdala (Senn et al. 2014) as competing inputs for subsequent cortical and subcortical processing.

To test the hypothesis that projections from the vHC and BLA compete for innervation of the mPFC, we analyzed structural changes in the projection from the BLA to mPFC in the NVHL rats. We found an increase in the density of "en passant" boutons in axons from the BLA projecting to the mPFC. As we show, these axons belong to CAMKII-expressing neurons, which use glutamate as their main neurotransmitter. Glutamatergic axonal boutons are highly dynamic structures (Krueger et al. 2003; Darcy et al. 2006) responsible for excitatory synapses (Shepherd and Harris 1998; Anderson and Martin 2001) that contribute to the remodeling of specific functional circuits in vivo (De Paola et al. 2006). Therefore, changes in their size and density reflect changes in synaptic activity (Schikorski and Stevens 1997; Murthy et al. 2001).

We analyzed the axonal boutons in 2 different areas of the mPFC: the IL and the PrL cortex. In agreement with previous studies, we show that the axons from the BLA innervate mainly Layers II and V of both IL and PrL areas (Gabbott et al. 2006). We found that NVHL produces an increase in axonal boutons in Layer II of both PrL and IL. It also produces an increase in Layer V of the PrL. Interestingly, when comparing NVHL and control animals, we observe an opposite effect in Layer V of the IL cortex: a decrease in the density of axonal boutons. Previous studies have shown that these 2 areas project to distinct populations within the amygdala (Vertes 2004; Gabbott et al. 2005). These 2 regions also play opposite functional roles: activation of PrL neurons increases fear expression whereas activation of IL projection

promotes extinction of fear (Vertes 2004; Gabbott et al. 2005; Gilmartin and McEchron 2005; Vidal-Gonzalez et al. 2006; Senn et al. 2014). Therefore, our results suggest that the opposite functional role of PrL and IL is reflected in differential density of boutons within the axons projecting from the BLA to specifically Layer V of these areas.

Several studies have quantified projecting neurons using retrograde tracers (Gabbott et al. 2005; Hale et al. 2008; Marchant et al. 2010, 2014; Vázquez-Borsetti et al. 2011). In the present study, we quantified and compared the intensity of the projection in terms of density of projecting neurons labeled with a retrograde tracer (Retrobeads) in the BLA after injecting in the IL/PrL cortex. In line with the results of the density of axonal boutons, we observed that NVHL animals have an increased density of labeled neurons. These data are consistent with the idea that the lesion leads to a disruption of the projection from the vHC to the mPFC, allowing an increase in the intensity of the projection from the BLA due to reduced competition for target innervation.

We further tested the hypothesis that synaptic activity of BLA neurons projecting to the mPFC is increased in NVHL rats, by using FosB as a marker of long-term activity (Hale et al. 2008; Marchant et al. 2010, 2014). Indeed, our data confirmed such increased activity in the projection from the BLA, showing that neurons from that region projecting to the mPFC of NVHL animals had higher FosB expression levels than control animals did.

Previous studies have shown that this particular lesion protocol produces a distinct behavioral phenotype in terms of anxiety and sensorimotor-gating tests (Lipska et al. 1995; Le Pen and Moreau 2002). Here, we replicate those results that have indicated that this protocol represents an animal model of schizophrenia (Lipska et al. 1993, 1995). Therefore, the disrupted balance between different projections that we find in our results might be the basis for at least some of the schizophrenic-like behaviors. This hypothesis is supported by the fact that we observed a correlation between the density of labeled neurons in the BLA and the reduction in the startle response. However, other brain areas projecting to the mPFC, such as the ventromedial and mediodorsal nuclei of the thalamus, might also compete for target innervation in the mPFC and should be studied as well in order to better understand the altered network configurations underlying cognition and emotions (Mitchell 2015; Timbie and Barbas 2015).

Taken together, these results support the idea that projections from the BLA and the vHC compete for target innervation in the mPFC through an activity-dependent mechanism during a time-window of high plasticity, in a manner analogous to that taking place in ocular dominance experiments in the visual cortex (Hubel and Wiesel 1970). Moreover, alterations during such sensitive period could lead to an abnormal network wiring, which might underlie the pathophysiology of neuropsychiatric disorders as schizophrenia.

Funding

This study was supported by ERC grant No 322742—iPLASTICITY, Sigrid Juselius foundation and Academy of Finland grant #257486. Funding to pay the Open Access publication charges for this article was provided by the European Research Council Advanced investigator grant.

Notes

Conflict of Interest: None declared.

References

Anderson JC, Martin K. 2001. Does bouton morphology optimize axon length? Nat Neurosci. 4:1166–1167.

Arnsten AF, Wang MJ, Paspalas CD. 2012. Neuromodulation of thought: flexibilities and vulnerabilities in prefrontal cortical network synapses. Neuron. 76:223–239.

Bacon SJ, Headlam AJ, Gabbott PL, Smith AD. 1996. Amygdala input to medial prefrontal cortex (mPFC) in the rat: a light and electron microscope study. Brain Res. 720:211–219.

Berardi N, Pizzorusso T, Maffei L. 2000. Critical periods during sensory development. Curr Opin Neurobiol. 10:138.

Carr DB, Sesack SR. 1996. Hippocampal afferents to the rat prefrontal cortex: synaptic targets and relation to dopamine terminals. J Comp Neurol. 369:1–15.

Corcoran KA, Desmond TJ, Frey KA, Maren S. 2005. Hippocampal inactivation disrupts the acquisition and contextual encoding of fear extinction. J Neurosci. 25:8978–8987.

Darcy KJ, Staras K, Collinson LM, Goda Y. 2006. Constitutive sharing of recycling synaptic vesicles between presynaptic boutons. Nat Neurosci. 9:315–321.

De Paola V, Holtmaat A, Knott G, Song S, Wilbrecht L, Caroni P, Svoboda K. 2006. Cell type-specific structural plasticity of axonal branches and boutons in the adult neocortex. Neuron. 49:861–875.

Fox K. 1992. A critical period for experience-dependent synaptic plasticity in rat barrel cortex. J Neurosci. 12:1826–1838.

Fuster JM. 2009. Cortex and memory: emergence of a new paradigm. J Cogn Neurosci. 21:2047–2072.

Gabbott P, Dickie B, Vaid R, Headlam A, Bacon S. 1997. Local-circuit neurones in the medial prefrontal cortex (areas 25, 32 and 24b) in the rat: Morphology and quantitative distribution. J Comp Neurol. 377:465–499.

Gabbott P, Headlam A, Busby S. 2002. Morphological evidence that CA1 hippocampal afferents monosynaptically innervate PV-containing neurons and NADPH-diaphorase reactive cells in the medial prefrontal cortex (Areas 25/32) of the rat. Brain Res. 946:314–322.

Gabbott PL, Warner TA, Busby SJ. 2006. Amygdala input monosynaptically innervates parvalbumin immunoreactive local circuit neurons in rat medial prefrontal cortex. Neuroscience. 139:1039–1048.

Gabbott PL, Warner TA, Jays PR, Salway P, Busby SJ. 2005. Prefrontal cortex in the rat: projections to subcortical autonomic, motor, and limbic centers. J Comp Neurol. 492:145–177.

Garcia R, Vouimba RM, Baudry M, Thompson RF. 1999. The amygdala modulates prefrontal cortex activity relative to conditioned fear. Nature. 402:294–296.

Geyer MA, Krebs-Thomson K, Braff DL, Swerdlow NR. 2001. Pharmacological studies of prepulse inhibition models of sensorimotor gating deficits in schizophrenia: a decade in review. Psychopharmacology. 156:117–154.

Gilmartin MR, McEchron MD. 2005. Single neurons in the medial prefrontal cortex of the rat exhibit tonic and phasic coding during trace fear conditioning. Behav Neurosci. 119:1496–1510.

Goldman-Rakic P, Schwartz M. 1982. Interdigitation of contralateral and ipsilateral columnar projections to frontal association cortex in primates. Science. 216:755.

Hale MW, Hay-Schmidt A, Mikkelsen JD, Poulsen B, Bouwknecht JA, Evans AK, Stamper CE, Shekhar A, Lowry CA. 2008. Exposure to an open-field arena increases c-Fos expression in a subpopulation of neurons in the dorsal raphe nucleus, including neurons projecting to the basolateral amygdaloid complex. Neuroscience. 157:733–748.

Harrison RV, Stanton SG, Ibrahim D, Nagasawa A, Mount RJ. 1993. Neonatal cochlear hearing loss results in developmental abnormalities of the central auditory pathways. Acta Otolaryngol. 113:296–302.

Hensch T. 2004. Critical period regulation. Ann Rev Neurosci. 27:549.

Hoover WB, Vertes RP. 2007. Anatomical analysis of afferent projections to the medial prefrontal cortex in the rat. Brain Struct Funct. 212:149–179.

Hubel D, Wiesel T. 1970. The period of susceptibility to the physiological effects of unilateral eye closure in kittens. J Physiol. 206:419.

Jay TM, Glowinski J, Thierry AM. 1989. Selectivity of the hippocampal projection to the prelimbic area of the prefrontal cortex in the rat. Brain Res. 505:337–340.

Ji J, Maren S. 2007. Hippocampal involvement in contextual modulation of fear extinction. Hippocampus. 17:749–758.

Kjelstrup KB, Solstad T, Brun VH, Hafting T, Leutgeb S, Witter MP, Moser EI, Moser M-BB. 2008. Finite scale of spatial representation in the hippocampus. Science. 321:140–143.

Krueger SR, Kolar A, Fitzsimonds RM. 2003. The presynaptic release apparatus is functional in the absence of dendritic contact and highly mobile within isolated axons. Neuron. 40:945–957.

Laviolette SR, Lipski WJ, Grace AA. 2005. A subpopulation of neurons in the medial prefrontal cortex encodes emotional learning with burst and frequency codes through a dopamine D4 receptor-dependent basolateral amygdala input. J Neurosci. 25:6066–6075.

Le Pen G, Moreau J-LL. 2002. Disruption of prepulse inhibition of startle reflex in a neurodevelopmental model of schizophrenia: reversal by clozapine, olanzapine and risperidone but not by haloperidol. Neuropsychopharmacology. 27:1–11.

Lee H, Dvorak D, Kao H-Y, Duffy Á, Scharfman H, Fenton A. 2012. Early cognitive experience prevents adult deficits in a neurodevelopmental schizophrenia model. Neuron. 75:714–724.

Levelt C, Hübener M. 2012. Critical-period plasticity in the visual cortex. Annu Rev Neurosci. 35:309–330.

Lipska B, Jaskiw G, Weinberger D. 1993. Postpubertal emergence of hyperresponsiveness to stress and to amphetamine after neonatal excitotoxic hippocampal damage: a potential animal model of schizophrenia. Neuropsychopharmacology. 9:67–75.

Lipska BK, Swerdlow NR, Geyer MA, Jaskiw GE, Braff DL, Weinberger DR. 1995. Neonatal excitotoxic hippocampal damage in rats causes post-pubertal changes in prepulse inhibition of startle and its disruption by apomorphine. Psychopharmacology. 122:35–43.

Marchant NJ, Furlong TM, McNally GP. 2010. Medial dorsal hypothalamus mediates the inhibition of reward seeking after extinction. J Neurosci. 30:14102–14115.

Marchant NJ, Rabei R, Kaganovsky K, Caprioli D, Bossert JM, Bonci A, Shaham Y. 2014. A critical role of lateral hypothalamus in context-induced relapse to alcohol seeking after punishment-imposed abstinence. J Neurosci. 34:7447–7457.

Mitchell AS. 2015. The mediodorsal thalamus as a higher order thalamic relay nucleus important for learning and decision-making. Neurosci Biobehav Rev. 54:76–88.

Murthy VN, Schikorski T, Stevens CF, Zhu Y. 2001. Inactivity produces increases in neurotransmitter release and synapse size. Neuron. 32:673–682.

Ressler KJ, Mayberg HS. 2007. Targeting abnormal neural circuits in mood and anxiety disorders: from the laboratory to the clinic. Nat Neurosci. 10:1116–1124.

Sandner G, Host L, Angst M-JJ, Guiberteau T, Guignard B, Zwiller J. 2011. The HDAC inhibitor phenylbutyrate reverses effects of neonatal ventral hippocampal lesion in rats. Front Psychiatry. 1:153.

Schikorski T, Stevens CF. 1997. Quantitative ultrastructural analysis of hippocampal excitatory synapses. J Neurosci. 17:5858–5867.

Senn V, Wolff S, Herry C, Grenier F, Ehrlich I, Gründemann J, Fadok J, Müller C, Letzkus J, Lüthi A. 2014. Long-range connectivity defines behavioral specificity of amygdala neurons. Neuron. 81:428–437.

Shepherd GM, Harris KM. 1998. Three-dimensional structure and composition of CA3 CA1 axons in rat hippocampal slices: implications for presynaptic connectivity and compartmentalization. J Neurosci. 18:8300–8310.

Sierra-Mercado D, Padilla-Coreano N, Quirk G. 2010. Dissociable roles of prelimbic and infralimbic cortices, ventral hippocampus, and basolateral amygdala in the expression and extinction of conditioned fear. Neuropsychopharmacology. 36: 529–538.

Sotres-Bayon F, Sierra-Mercado D, Pardilla-Delgado E, Quirk G. 2012. Gating of fear in prelimbic cortex by hippocampal and amygdala inputs. Neuron. 76:804–812.

Spellman T, Rigotti M, Ahmari SE, Fusi S, Gogos JA, Gordon JA. 2015. Hippocampal-prefrontal input supports spatial encoding in working memory. Nature. 522:309–314.

Strange BA, Witter MP, Lein ES, Moser EI. 2014. Functional organization of the hippocampal longitudinal axis. Nat Rev Neurosci. 15:655–669.

Tierney P, Dégenètais E, Thierry A-M, Glowinski J, Gioanni Y. 2004. Influence of the hippocampus on interneurons of the rat prefrontal cortex. Eur J Neurosci. 20:514.

Timbie C, Barbas H. 2015. Pathways for Emotions: Specializations in the amygdalar, mediodorsal thalamic, and posterior orbitofrontal network. J Neurosci. 35:11976–11987.

Toth M, Tulogdi A, Biro L, Soros P, Mikics E, Haller J. 2012. The neural background of hyper-emotional aggression induced by post-weaning social isolation. Behav Brain Res. 233:120–129.

Van der Loos H, Woolsey TA. 1973. Somatosensory cortex: structural alterations following early injury to sense organs. Science. 179:395–398.

Vázquez-Borsetti P, Celada P, Cortés R, Artigas F. 2011. Simultaneous projections from prefrontal cortex to dopaminergic and serotonergic nuclei. Int J Neuropsychopharmacol. 14: 289–302.

Vertes RP. 2004. Differential projections of the infralimbic and prelimbic cortex in the rat. Synapse. 51:32–58.

Vidal-Gonzalez I, Vidal-Gonzalez B, Rauch SL, Quirk GJ. 2006. Microstimulation reveals opposing influences of prelimbic and infralimbic cortex on the expression of conditioned fear. Learn Mem. 13:728–733.